

Deep Photo Scan: Semi-supervised learning for dealing with the real-world degradation in smartphone photo scanning

Man M. Ho
Hosei University
Tokyo, Japan

man.hominh.6m@stu.hosei.ac.jp

Jinjia Zhou
Hosei University
Tokyo, Japan

jinjia.zhou.35@hosei.ac.jp



Figure 1. We present the DIV2K-SCAN dataset for smartphone-scanned photo restoration and propose the semi-supervised Deep Photo Scan (DPScan). As a result, our work outperforms the recent academic research Old Photo Restoration [34] and industrial products Google Photo Scan and Genius Scan in smartphone photo scanning.

Abstract

Physical photographs now can be conveniently scanned by smartphones and stored forever as a digital version, but the scanned photos are not restored well. One solution is to train a supervised deep neural network on many digital photos and the corresponding scanned photos. However, human annotation costs a huge resource leading to limited training data. Previous works create training pairs by simulating degradation using image processing techniques. Their synthetic images are formed with perfectly scanned photos in latent space. Even so, the real-world degradation in smartphone photo scanning remains unsolved since it is more complicated due to real lens defocus, lighting conditions, losing details via printing, various photo materials, and more. To solve these problems, we propose a Deep Photo Scan (DPScan) based on semi-supervised learning. First, we present the way to produce real-world degradation and provide the DIV2K-SCAN dataset for smartphone-scanned photo restoration. Second, by using DIV2K-SCAN, we adopt the concept of Generative Adversarial Networks to learn how to degrade a high-quality image as if it were scanned by a real smart-

phone, then generate pseudo-scanned photos for unscanned photos. Finally, we propose to train on the scanned and pseudo-scanned photos representing a semi-supervised approach with a cycle process as: high-quality images \rightarrow real/pseudo-scanned photos \rightarrow reconstructed images. The proposed semi-supervised scheme can balance between supervised and unsupervised errors while optimizing to limit imperfect pseudo inputs but still enhance restoration. As a result, the proposed DPScan quantitatively and qualitatively outperforms its baseline architecture, state-of-the-art academic research, and industrial products in smartphone photo scanning. Our work is available at <https://minhmanho.github.io/dpscan>.

1. Introduction

Every moment passing by is precious; especially, when it marks important life events such as graduation, wedding. The moments are usually captured in photographs. However, we do not always have a digital version since digital cameras were not commonly used in the past, or we accidentally lost it. Thanks to technological development, photographs can now be efficiently stored as a high-

resolution digital image scanned just by a smartphone. It also provides an efficient way to share the captured moments in physical photographs to everyone through the internet. To restore the scanned photos, the recent Old Photo Restoration (OPR) [33, 34] based on Deep Neural Networks (DNNs) tries to mimic and learn the scanning degradation using low-level image processing techniques such as Gaussian Noise, Gaussian Blur. Their artificially degraded photos are then formed with the perfectly scanned old photos in latent space. However, the smartphone-scanned photos are still not restored well since they contain more complicated degradation caused by real lens defocus, lighting conditions, various photo materials, losing details via printing, photo size, etc. In this work, we adopt DIV2K [32] and present the DIV2K-SCAN dataset providing the real-world degradation in smartphone photo scanning. Furthermore, we leverage the concept of Generative Adversarial Networks (GANs) [8, 15, 47] to learn how to create the real smartphone-scanned photos treated as pseudo inputs for training. Being joint with supervised training, we create a cycle process as high-quality images \rightarrow scanned photos/pseudo inputs \rightarrow reconstructed images. The proposed semi-supervised scheme can balance between supervised and unsupervised errors while optimizing to enhance restoration but not let the trained model out-of-control caused by imperfect pseudo inputs.

Creating real-world degradation for training. The performance of DNNs mostly depends on how the training data is created. So it is crucial to create a specific degradation that is close to real-world problems. For example, [32, 36, 6, 18] use traditional interpolation techniques to achieve the distortion representing the problem of super-resolution. However, they result in distortion and lost details for digital zooming. [45] thus presented a way to obtain ground-truth for zoomed regions by optically zooming and provide a dataset for real-world computational zoom. Their work thus outperforms the state-of-the-art super-resolution [36] in the field. It has the same motivation as [27, 1] solving the real noise of photographs caused by low-ISO, [14] enhancing smartphone-taken photos by creating training {smartphone, DSLR camera} pairs. In this work, it is the first time to have a dataset (DIV2K-SCAN) that provides real-world degradation for smartphone-scanned photo restoration. This dataset is then utilized to learn the degradation and generate pseudo inputs for unscanned high-quality images in semi-supervised training.

Detecting the contour of scanned photos. Before perspective warping transforming a smartphone-scanned photo to have a bird's-eye view, the scanned photo's contour needs to be identified, as shown in Figure 2. The traditional edge detection techniques [4, 17] achieve a real-time performance to find the contour of interests. However, they still suffer from complicated cases having similar

colors between the scanned photo and background, leading to the scanned photo's incomplete contour, as visualized in our supplemental document. [39, 9, 23, 28] proposed DNN-based edge detection methods and achieved much better performance. However, these methods require a long processing time. To address this problem, we leverage both traditional [4] with opening morphing noise reduction and DNN-based [28] techniques for our contour detection method, which can greatly reduce the processing time. In production, when detecting contour of interests goes wrong, the users with touchscreen-equipped smartphones can easily correct the contour.

Semi-supervised learning for exploiting the infinite number of unscanned high-quality images. Since the human-annotated data costs a considerable resource, worldwide researchers have proposed many semi-supervised learning techniques to solve the problem of lacking labeled data (ground-truth) while training a deep neural network. For example, the image classification works [3, 40, 5] utilized a well-trained model (teacher) to generate pseudo labels for unlabeled images that the smaller network (student) can be trained on them. The semantic segmentation work [26] added an unsupervised loss on synthetic maps predicted by auxiliary decoders for unlabeled samples. They all provided good schemes when the ground-truth data is limited. However, for this work, we lack the input data for training. Thanks to the seminal work of Generative Adversarial Networks (GANs) [8], the synthetic images now are high-fidelity and closer to the target distribution [15]. Moreover, the synthetic images can be translated back to the input domain, creating a cycle consistency [47, 37] for the task. Inspired by the mentioned works, we adopt the concept of GANs to simulate smartphone-scanned photos and degrade unscanned images, then provide them as pseudo inputs for unsupervised training. Being joint with supervised training, it will create a cycle fashion as high-quality images \rightarrow scanned photos/pseudo inputs \rightarrow reconstructed images, as shown in Figure 2. The proposed semi-supervised scheme balances between supervised and unsupervised errors while optimizing to enhance restoration but not let the trained model out-of-control caused by imperfect pseudo inputs.

Network architecture. The autoencoder architecture U-Net [29] and its variants have gained high performance and become well-known in image-to-image translation tasks [2, 44, 15, 12]. Developing along with the field, many techniques for customizing the components of a deep neural network have also grown rapidly towards enhancing efficiency and effectiveness. It is meaningful to this smartphone photo scanning to operate on a limited resource. Inspired by the attention mechanism, the Efficient Channel Attention (ECA) [35] module reduces a huge computational cost with good performance compared to its backbones in

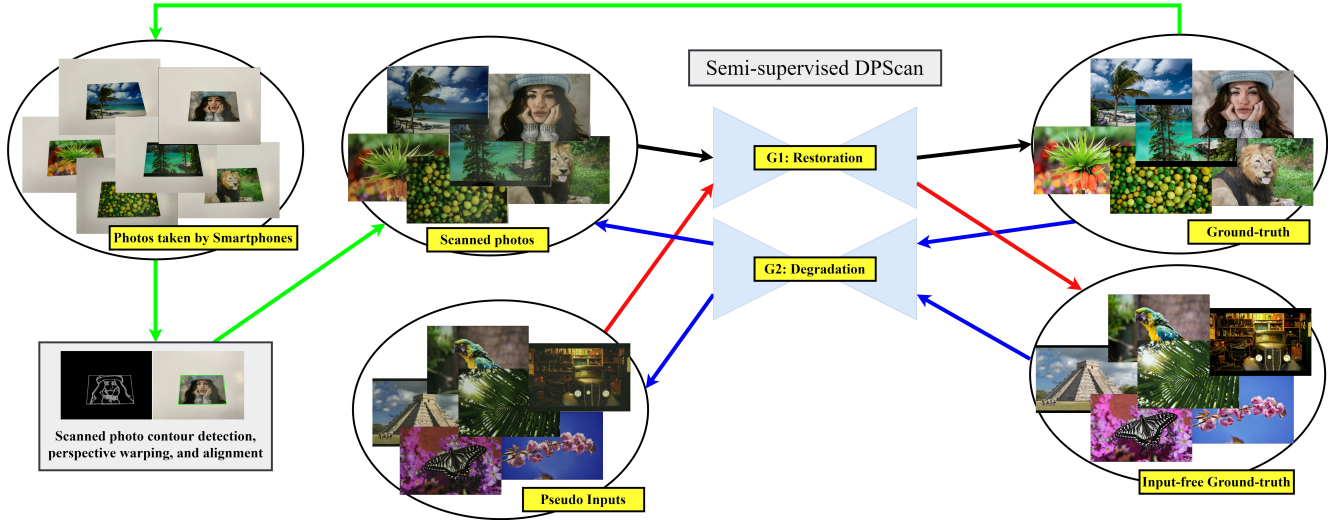


Figure 2. A summary of our semi-supervised Deep Photo Scan (DPScan). We produce real-world degradation by printing the ground-truth images, taking the digital version of printed photos using a smartphone, perspective warping, and aligning them (green). However, that process costs a huge resource. To overcome this issue, in training, G2 learns to degrade the ground-truth images as being scanned and synthesize pseudo inputs for input-free ground-truth images (blue). Therefore, our G1 can learn to restore on more contexts in supervised (black) and unsupervised (red) ways representing a semi-supervised approach for smartphone-scanned photo restoration.

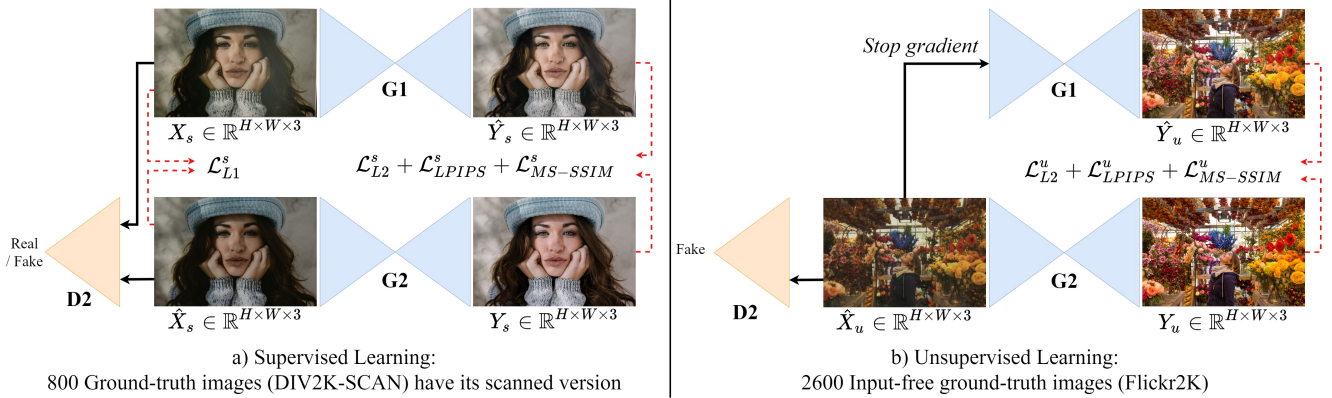


Figure 3. We present a semi-supervised learning that enables our restoration to be trained on scanned (supervised) (a) and unscanned (unsupervised) (b) photos under strong similarity loss functions such as $L2$ (\mathcal{L}_{L2}^*), LPIPS [43] (\mathcal{L}_{LPIPS}^*), and MS-SSIM [38] ($\mathcal{L}_{MS-SSIM}^*$), where $*$ denotes s or u representing supervised or unsupervised scheme respectively. Meanwhile, the distribution of real-scanned photos is captured with adversarial losses and $L1$ (\mathcal{L}_{L1}^s). Errors between (a) and (b) are balanced while optimization.

image classification, object detection, and semantic segmentation. Therefore, in this work, we leverage ECA to design a Residual ECA (RECA) Block and RECA U-Block for our restoration task. As a consequence, the customized blocks show the capability of enhancing performance in image restoration and outperforms its baseline (so-called simple DPScan) consisting of U-Net [29], residual modules [16] between encoder and decoder, anti-aliasing blur pooling [42], EvoNorm-S0 [22].

Our contributions are as follows:

- We present the DIV2K-SCAN dataset providing real-world degradation in smartphone photo scanning. A

result shows that a simple supervised model trained on our dataset can outperform the previous work trained on the simulated degradation.

- Based on DIV2K-SCAN, we adopt the concept of GAN to learn how to degrade a high-quality image as if it were scanned by a smartphone. Hence, we can utilize an unlimited number of unscanned high-quality images on the internet for training.
- We propose semi-supervised Deep Photo Scan (DP-Scan) having two advantages: 1) semi-supervised approach training on both scanned and unscanned photos, and 2) the designed Residual Efficient Channel At-

tention (RECA) Block and RECA U-Block based on ECA [35]. As a result, our semi-supervised DPScan outperforms its baseline, the previous research work, and industrial products quantitatively and qualitatively in smartphone-scanned photo restoration.

2. The Proposed Deep Photo Scan (DPScan)

Our work consists of two main components: (1) data preparation consisting of reproducing real-world degradation and simulating professional scanner, and (2) the proposed semi-supervised DPScan for smartphone-scanned photo restoration.

Regarding (1), we leverage both traditional Canny [4] and DNN-based [28] edge detection techniques to identify the contour of interests. Afterward, the annotated-scanned images are perspectively warped and cropped to have a bird’s-eye view as if a professional scanner scans it. Furthermore, we apply a precise alignment based on SIFT [24] and RANSAC [7, 31] to suppress the structural mismatch between inputs and ground-truth images, as highlighted in Figure 2.

The framework of our semi-supervised DPScan (2) includes two generators $G1$, $G2$, and a discriminator $D2$. Particularly, $G1$ restores scanned photos and is trained under supervised loss functions. Meanwhile, the GAN-based $G2$ provides the pseudo inputs for unscanned photos and is trained with the discriminator $D2$, distinguishing between the real and fake scanned photo. Initially, all models are pre-trained on DIV2K-SCAN with supervised learning, and $G1$ is trained independently with $G2$ and $D2$. Afterward, $G1$, $G2$, and $D2$ are jointly trained on scanned photos from DIV2K-SCAN and unscanned photos from Flick2K [32], representing a semi-supervised approach dealing with the lack of inputs, as shown in Figures 2 and 3.

Regarding network architecture, we adopt U-Net [29], which have been proved its proficiency in various image-to-image translation tasks, residual modules [10], blur pooling [42], and EvoNorm-S0 [22] to design our $G1$ and $G2$. To enhance $G1$ in generating a very detailed photo with efficiency, we leverage the Efficient Channel Attention (ECA) [35] module to design Residual ECA (RECA) Block and RECA U-Block for the more efficient but effective in this restoration task. Besides, we utilize the discriminator of SA-GAN [41] with Spectral Normalization [25] as our $D2$.

2.1. Supervised learning for pre-training $G1$ independently to $G2$ and $D2$

In pre-training on DIV2K-SCAN with supervised learning, after perspective warping, our $G1 : X \rightarrow Y$ restores the scanned inputs $X_s \in \mathbb{R}^{H \times W \times 3}$ to have $\hat{Y}_s \in \mathbb{R}^{H \times W \times 3}$, as follows:

$$\hat{Y}_s = G1(X_s) \quad (1)$$

The errors between $\hat{Y}_s \in \mathbb{R}^{H \times W \times 3}$ and its ground-truth images Y are optimized under several supervised losses such as $L2$, Multiscale Structural Similarity (MS-SSIM) [38], and the perceptual distance LPIPS [43] as follows:

$$\mathcal{L}_{G1}^s = \alpha * \mathcal{L}_{L2}^s + \beta * \mathcal{L}_{LPIPS}^s + \gamma * \mathcal{L}_{MS-SSIM}^s \quad (2)$$

where:

$$\mathcal{L}_{L2}^s = \|Y_s - \hat{Y}_s\|_2^2,$$

$$\mathcal{L}_{MS-SSIM}^s = MS-SSIM(Y_s, \hat{Y}_s) \text{ described in [38],}$$

$$\mathcal{L}_{LPIPS}^s = LPIPS(Y_s, \hat{Y}_s) \text{ described in [43].}$$

To learn the specific degradation of scanned photos from the DIV2K-SCAN, we independently train a simply-designed network $G2 : Y \rightarrow X$ to degrade the ground-truth images Y_s to synthesize its scanned version $\hat{X}_s \in \mathbb{R}^{H \times W \times 3}$, as follows:

$$\hat{X}_s = G2(Y_s) \quad (3)$$

Instead of conditioning discriminator [25, 41], we train the generator $G2$ and discriminator $D2$ under the $L1$ [15] and hinge adversarial losses [20] as:

$$\begin{aligned} \mathcal{L}_{D2}^s = & -\mathbb{E}_{X_s}[\min(0, -1 + D(X_s))] \\ & - \mathbb{E}_{Y_s}[\min(0, -1 - D(G2(Y_s)))] \end{aligned} \quad (4)$$

$$\mathcal{L}_{G2}^s = -\mathbb{E}_{Y_s}[D(G2(Y_s))] \quad (5)$$

$$\mathcal{L}_{L1}^s = \mathbb{E}_{X_s, Y_s}[\|X_s - G2(Y_s)\|_1] \quad (6)$$

The total loss for $G2$ is defined as:

$$\mathcal{L}_{G2}^{s, final} = \alpha * \mathcal{L}_{L1}^s + \delta * \mathcal{L}_{G2}^s \quad (7)$$

We empirically set $\alpha = 1$, $\beta = 0.2$, and $\gamma = 1$, $\delta = 0.05$ for this supervised learning scheme.

2.2. Semi-supervised learning for fine-tuning $G1$, $G2$, and $D2$ together

After pre-training on DIV2K-SCAN, we then train $G1$, $G2$, and $D2$ together on both DIV2K-SCAN providing the ground-truth images Y_s with their scanned photos X_s and Flick2K [32] providing the input-free ground-truth images $Y_u \in \mathbb{R}^{H \times W \times 3}$.

Firstly, X_s and Y_s are processed as described in Section 2.1. Secondly, $G2$ provides pseudo inputs \hat{X}_u for Y_u as:

$$\hat{X}_u = G2(Y_u) \quad (8)$$

under adversarial losses updated from Equations 4 and 5 as:

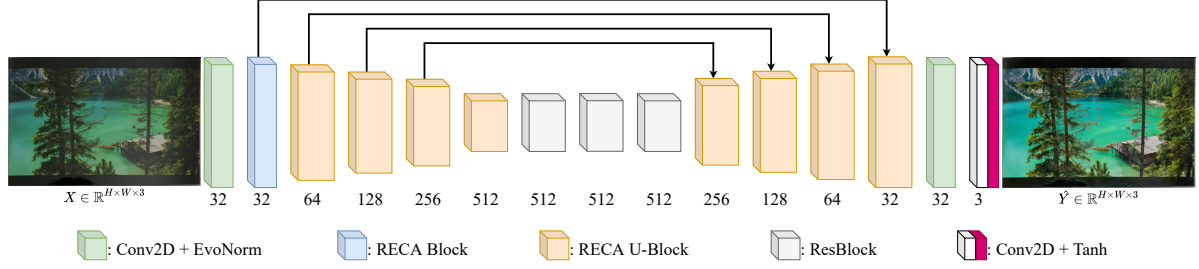


Figure 4. Our deep neural network for $G1$ restoring the scanned photo X to have its high-quality \hat{Y} .

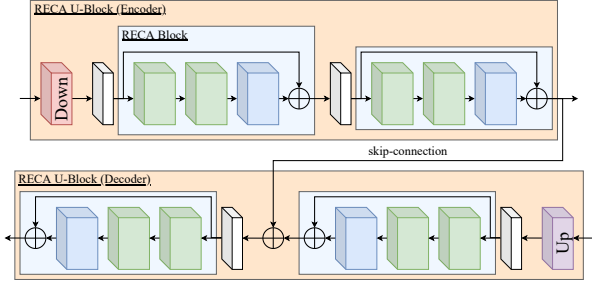


Figure 5. Illustrations for Residual Efficient Channel Attention (RECA) Block and RECA U-Block based on ECA [35]. Regarding "DOWN"-sampling and "UP"-sampling, we use the anti-aliasing max pooling and bi-linear interpolation from [42]. \oplus represents a summation.

$$\begin{aligned} \mathcal{L}_{D2} = & -\mathbb{E}_{X_s} [\min(0, -1 + D(X_s))] \\ & - 0.5 * (\mathbb{E}_{Y_s} [\min(0, -1 - D(G2(Y_s)))] \\ & + \mathbb{E}_{Y_u} [\min(0, -1 - D(G2(Y_u)))] \end{aligned} \quad (9)$$

$$\begin{aligned} \mathcal{L}_{G2} = & -0.5 * (\mathbb{E}_{Y_s} [D(G2(Y_s))]) \\ & + \mathbb{E}_{Y_u} [D(G2(Y_u))] \end{aligned} \quad (10)$$

Combined with the supervised loss in Equation 6, we have the updated total loss for $G2$ as:

$$\mathcal{L}_{G2-final} = \alpha * \mathcal{L}_{L1}^s + \delta * \mathcal{L}_{G2} \quad (11)$$

Afterward, $G1$ leverages the pseudo input \hat{X}_u to synthesize the reconstructed \hat{Y}_u creating a cycle fashion as:

$$\hat{Y}_u = G1(sg(\hat{X}_u)) = G1(sg(G2(Y_u))) \quad (12)$$

where sg denotes the *stop-gradient* function added to avoid falsifying the distribution of real-scanned photos. Similar to Equation 2, the defined loss function for $G1$ optimizing errors between \hat{Y}_u and Y_u is as:

$$\mathcal{L}_{G1}^u = \alpha * \mathcal{L}_{L2}^u + \beta * \mathcal{L}_{LPIS}^u + \gamma * \mathcal{L}_{MS-SSIM}^u \quad (13)$$

Finally, the semi-supervised loss function for $G1$ is as:

$$\mathcal{L}_{G1} = \eta * \mathcal{L}_{G1}^s + (1 - \eta) * \mathcal{L}_{G1}^u \quad (14)$$

where η is a balance weight between supervised and unsupervised errors, and is set to 0.5. Other hyper-parameters empirically re-set $\alpha = 1$, $\beta = 0.1$, and $\gamma = 0.25$, $\delta = 0.05$ for this semi-supervised learning scheme.

2.3. Network architecture

The proposed semi-supervised DPScan consists of three main deep neural networks: $G1 : X \rightarrow Y$ for scanned photo restoration, $G2 : Y \rightarrow X$ for degrading high-quality images, and discriminator $D2$ trained belongs with $G2$ to distinguish whether the generated images are in the real-scanned photos domain or not.

Generator $G1$ is designed based on the network architecture of U-Net [29] with skip connections [12], residual modules (ResBlock) between the encoder and decoder [10, 16], EvoNorm-S0 [22], which have achieved a high performance in image-to-image translation tasks. The network architecture adopting the mentioned techniques is named simple DPScan. Besides, in each block of the encoder and decoder, we leverage the anti-aliasing max pooling and bi-linear interpolation [42] for our down-sampling and up-sampling, respectively. Besides, the Efficient Channel Attention (ECA) module [35], which has shown the efficiency but effectiveness in image classification, is adopted to design Residual ECA (RECA) and RECA U-Block, as described in Figures 4 and 5. The final network architecture is so-called DPScan. Please check our supplemental document for the technical details.

Generator $G2$ and Discriminator $D2$. We utilize the simple network architecture (simple DPScan) for $G2$ to generate pseudo-scanned photos. Meanwhile, $D2$ is entirely based on the discriminator of SA-GAN [41] with Spectral Normalization [25]. Please check our supplemental document for more details.

2.4. Data preparation and DIV2K-SCAN

Generating the real-world degradation. We first rotate the high-quality images from DIV2K [32] 90 degrees to the

left when their width is smaller than height, and centrally crop all images with a ratio of 15 : 10. Afterward, we ask a professional photography lab to print the processed images out with a size of $7.5\text{cm} \times 5\text{cm}$ each. All physical photos are then digitally taken in a room with sufficient light intensity on the white background using iPhone XR. Therefore, our generated samples are highly characteristic for training and test with the glare by lighting sources reflecting on the physical photo, smartphone-camera defocuses, structural distortion while taking in the 3D world, missing details due to scaling for printing, etc.

Contour detection and image alignment. After achieving the digital images of printed photos, we apply the efficient Canny [4] edge detection to detect the contours of the actual scanned photos in the white background. However, the method is sensitive to the color between the boundary and usually makes mistakes in detecting a closed contour. Thus, we utilize DexiNed [28], which achieved state-of-the-art performance in the field, to support Canny’s method. Humans will manually correct the remaining failed contour detection. Please check our supplemental document for discussion and visualization.

Even though the bird’s-eye view is obtained, the structural mismatch between the warped images and its ground-truth still occurs. It becomes more challenging to train a deep neural network. The recent work RANSAC-flow [30] presents an advanced technique to precisely align an image to another one having the same context; however, our precious degradation is influenced by their interpolation. To reduce structural mismatch while the degradation remaining intact, we leverage the SIFT features [24] and RANSAC [7, 31] to align the warped images to their ground-truth precisely. We eventually achieve 900 ground-truth images with its scanned version for supervised training, validation, and test.

Training data. We trained our models on 800 scanned images from DIV2K-SCAN and 2,600 unscanned images from Flickr2K [19]. Since the printed photos might lose details at their boundary because of mistakes in cutting photographs, we thus centrally crop training images to the size of 90% of the total size, then resize the images to 1080×720 for training. While training, the data is augmented by a random crop with a size of 384×384 , randomly flip in both horizontal and vertical ways, and randomly rotate with the degrees 0, 90, 180, 270.

Validation and test data. We divide the remaining 100 images from DIV2K-SCAN to 40% for validation (*valset*) and 60% for test (*testset*). All sets are resized to 1072×720 . Since Google Photo Scan has an automatic alignment with inappropriate cropping causing lost information at borders, we thus additionally evaluate the works on centrally-cropped *valset* and *testset* with the size of 75% of the total size, so-called *valset 75* and *testset 75*.

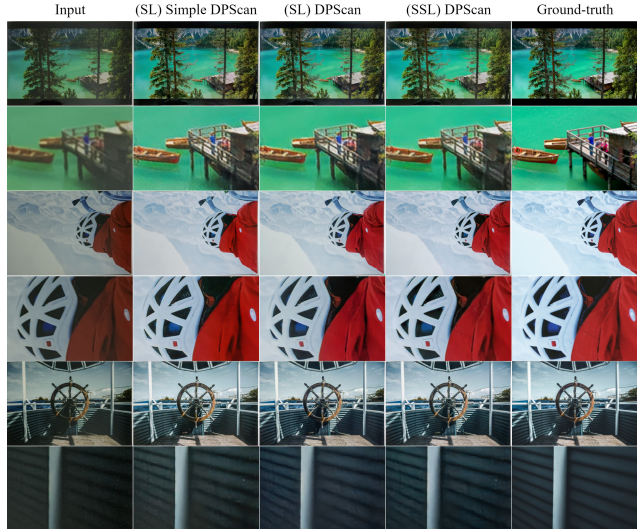


Figure 6. Qualitative comparison between our supervised (SL) models without (simple DPScan)/with (DPScan) the designed RECA and RECA U-Block, and our semi-supervised (SSL) DPScan. **Better when zoomed in.**

Table 1. Quantitative comparison to the industrial products Google Photo Scan (GPS), Genius Scan (GS), the previous work Old Photo Restoration (OPR) [34], the supervised (SL) Pix2Pix [15], supervised CycleGAN [47], our supervised DPScan without (simple)/with the designed RECA and RECA U-Block scheme, and our semi-supervised (SSL) DPScan. **Bold** values represent the highest performance in PSNR \uparrow , LPIPS \downarrow [43], and MS-SSIM \uparrow [38]. \uparrow denotes higher is better, and vice versa.

Method	75% Centrally Cropped			Full Size		
	PSNR \uparrow	LPIPS \downarrow	MS-SSIM \uparrow	PSNR \uparrow	LPIPS \downarrow	MS-SSIM \uparrow
GPS	16.48	0.3637	0.8374	14.20	0.4202	0.7881
GS	16.35	0.3713	0.8155	15.44	0.3969	0.7873
OPR [34]	18.50	0.2934	0.8349	17.09	0.3231	0.8043
(SL) Pix2Pix [15]	20.65	0.2589	0.8679	18.87	0.2951	0.8303
(SL) CycleGAN [47]	17.27	0.3300	0.8335	16.28	0.3572	0.8025
(SL) Simple DPScan	21.67	0.1801	0.8899	19.17	0.2120	0.8502
(SL) DPScan	22.18	0.1656	0.8959	19.43	0.1965	0.8551
(SSL) DPScan	22.30	0.1690	0.8959	19.47	0.1963	0.8542

3. Experiments

This section reveals our technical implementation and ablation studies on the network architecture and learning approach (please check our supplemental documents for the ablation studies on preprocessing techniques for training data). Moreover, we compare our DPScan to the previous works including (1) **Industrial products Google Photo Scan (GPS) and Genius Scan (GS)**. We use these applications to produce their results manually. (2) **Academic research Old Photo Restoration [34]** degrading high-quality images using low-level image processing techniques and making it more *perfectly scanned* and *older* in latent space. (3) The typical works, **Pix2Pix [15]** and **CycleGAN [47]**, that achieve high performance in image-to-image translation tasks. To be fair, we retrain them in the same supervised learning condition described in Section 2.1.

All comparisons are qualitative and quantitative conducted on DIV2K-SCAN valset and testset described in Section 2.4 using similarity metrics such as Peak Signal-to-Noise Ratio (PSNR), LPIPS [43], and MS-SSIM [38]. Despite experimenting on both full images and cropped images retaining 75% of the original size, we mainly discuss results produced from the cropped images for fair comparisons to the industrial products. Additionally, we conduct a user study based on two-alternative forced-choice (2AFC) to compare all methods’ performance in scanned photo restoration subjectively.

3.1. Ablation study on the network architecture and learning approach

We adopt U-Net [29], residual modules [10, 16], anti-aliasing down-/up-samplers [42], EvoNorm [22] to design a base architecture, so-called simple DPScan. While considering improving network architecture, we conduct an ablation study on customized deep learning techniques such as Flow Warping Block (FWB) [13], Residual Feature-based Attention (RFA), Residual Self-Attention (RSA) [41], Residual Channel Attention Block (RCAB) [46], and Residual Efficient Channel Attention (RECA) [35]. The Efficient Channel Attention (ECA) [35] has shown the efficiency but effectiveness in reducing computational costs with high accuracy for the image classification task. Moreover, an experimental result shows that the customized RECA outperforms other ablation techniques with the best image quality (please check our supplemental document for technical and experimental details). Therefore, we leverage the RECA module and its variant RECA U-Block to design our network, as shown in Figures 4 and 5. The improved architecture is called DPScan. To judge the entire improvement of DPScan, we compare it to the simple DPScan by training and evaluating them in the same supervised learning condition described in Section 2.1. Besides, we conduct a comparison between our supervised and semi-supervised DPScan to prove the proficiency of our semi-supervised framework learning on scanned and unscanned images. As a qualitative result, our supervised DPScan outperforms its simple version in restoring edges with fewer artifacts. Although the performance has been improved, there remains *glare*, *distorted edges* in the first sample, *blurry details* in the second and third samples, likely being overlaid by a gray layer with the opacity of 50%. By training on more unscanned photos, the semi-supervised DPScan can generate fewer artifacts with clearer edges, as the *fence* in the first sample, *pillar* in the third sample shown in Figure 6. Furthermore, the glare effect caused by smartphone photo scanning is suppressed in the second and third samples. Quantitatively, the supervised DPScan entirely outperforms its simple version with the better (PSNR, LPIPS, MS-SSIM) as (22.18, 0.1656, 0.8959). Beyond supervised learning, the

semi-supervised DPScan provides the better PSNR compared to its supervised version with higher PSNR as **22.30 dB** on *testset 75*. The unstable outperformance in LPIPS and MS-SSIM is discussed in our user study section and supplemental document.

3.2. Comparison to the previous work and industrial products

Industrial products Google Photo Scan (GPS) and Genius Scan (GS) provide distorted results with significant artifacts. Inspired by deep learning, Old Photo Restoration (OPR) [34] trained their networks on the scanning degradation simulated by low-level image processing techniques. Although their synthetic images are formed with the perfectly real-scanned old photos in latent space, their model is weakly trained because the ground-truth images of real-scanned photos are missing. Furthermore, the real-world degradation in smartphone photo scanning is more complicated caused by real lens defocus, lighting conditions, various photo materials, losing details due to scaling for printing, etc. To overcome this issue, we present the DIV2K-SCAN dataset providing real-world degradation for smartphone-scanned photo restoration. Furthermore, taking advantage of ECA [35], we design a specific deep neural network with RECA Block and RECA U-Block, named DPScan. Additionally, a semi-supervised approach is proposed to exploit an unlimited number of unscanned high-quality images by providing pseudo-scanned photos. Our semi-supervised DPScan is thus more robust than its supervised model. As a quantitative result, although GPS is worse than the GS on full-size images because of its post-processing cropping, GPS has a better restoration on cropped images. The deep-learning-based OPR [34] has show their effectiveness as outperforming the industrial GPS and GS with better (PSNR, LPIPS, MS-SSIM) as (18.5, 0.2934, 0.8349) on *testset 75*. Being trained on our DIV2K-SCAN, two supervised models Pix2Pix [15] and the proposed DPScan can outperform OPR [34] in solving the real degradation. Although the traditional Pix2Pix [15] and CycleGAN [47] provide interesting ways to capture data distribution with adversarial losses, they are worse than our supervised DPScan proving the effectiveness of supervised learning in synthesizing a very detailed photo. Beyond supervised learning, our semi-supervised DPScan trained on more unscanned images shows the higher performance than the compared works, especially its supervised version, with better (PSNR, LPIPS, MS-SSIM) as (22.30, 0.1690, 0.8959) on *testset 75*, as shown in Table 1. Qualitatively, the semi-supervised DPScan generates great details without glare. Particularly, our results have the most detailed *girl*, *bird*, *lines*, *bookcases*, *car* in *top-down order*, as shown in Figure 7. We conclude that our semi-supervised DPScan outperforms the previous works in both quantita-



Figure 7. Qualitative comparison between two industrial products Google Photo Scan (GPS), Genius Scan (GS), the previous work Old Photo Restoration (OPR) [34], two traditional works Pix2Pix [15], CycleGAN [47] trained on DIV2K-SCAN, and our semi-supervised DPScan. Ours produces the most detailed photos without glare and color fading. **Better when zoomed in.**

tive and qualitative ways. Please check our supplemental document for more qualitative results and a comparison to CycleGAN [47] on degrading high-quality images.

3.3. Out-of-distribution

This work intends to solve a specific case of smartphone-scanned photo restoration. Our training and test sets are therefore captured in the same condition. However, the input distribution is more complicated in practice. Particularly, while scanning photographs in nature, the lightning condition affects the taken color; meanwhile, mobile devices such as lenses and sensors affect the captured details, causing distorted edges and compression noises. Besides,

each smartphone has its photo post-processing, diversifying the real-world degradation. Hence, an experiment on out-of-distribution (OOD) is crucial to judge our work at the industrial level. We prepare two test sets having different distribution from our DIV2K-SCAN by (i) changing color using Simplest Color Balance (SCB) [21] and (ii) capturing another testset using Xperia XZ1. SCB [21] can improve the quality of DIV2K-SCAN; meanwhile, photos scanned by Xperia XZ1 are worse than DIV2K-SCAN scanned by iPhone XR. As a result, our work still shows its effectiveness in scanned photo restoration and quantitatively outperforms Pix2Pix [15], CycleGAN [47], and Old Photo Restoration [34], as described in Table 2. Subjec-

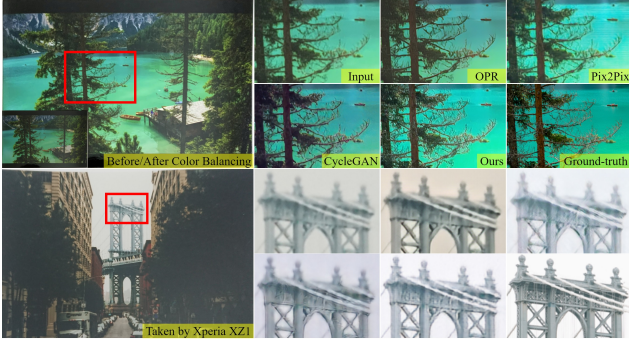


Figure 8. Qualitative comparison in case of out-of-distribution including the color-balanced [21] testset (top) and the testset taken by Xperia XZ1 (bottom). Ours still obtains a high performance in restoring smartphone-scanned photos. **Better when zoomed in.** Check our supplemental document for more results.

Table 2. Quantitative comparisons in case of out-of-distribution (OOD) using PSNR \uparrow , LPIPS \downarrow , and MS-SSIM \uparrow . We generate and compare two OOD testsets by (i) applying Simplest Color Balance (SCB) [21] on DIV2K-SCAN testset and (ii) taking the new testset with Xperia XZ1, and estimate the base scores as in (a). Afterward, we compare our work to Pix2Pix [15], CycleGAN [47], Old Photo Restoration (OPR) [34] on the quality improvement anchored by the base scores corresponding to each testset as in (b). the. As a result, our work still shows the effectiveness in scanned-photo restoration and obtains the best performance as **bold** values in (b). \uparrow : higher is better, and vice versa.

(a) OOD testset 75 (centrally cropped to 75% of the total size)				PSNR \uparrow	LPIPS \downarrow	MS-SSIM \uparrow
Testset 75				16.41	0.3711	0.8177
DIV2K-SCAN				18.97	0.3475	0.8578
DIV2K-SCAN + SCB [21]				14.81	0.4354	0.7285
Xperia XZ						

(b) Comparison on OOD testset 75						
Method	DIV2K-SCAN + SCB [21]			Xperia XZ1		
	Δ PSNR \uparrow	Δ LPIPS \downarrow	Δ MS-SSIM \uparrow	Δ PSNR \uparrow	Δ LPIPS \downarrow	Δ MS-SSIM \uparrow
OPR[34]	-0.35	-0.06	-0.01	3.15	-0.09	0.06
Pix2Pix[15]	0.67	-0.08	0.01	2.61	-0.07	0.05
CycleGan[47]	-0.44	-0.09	-0.01	2.62	-0.11	0.07
Ours	1.37	-0.15	0.03	4.47	-0.15	0.09

tively, our semi-supervised DPScan provides very detailed photos in both OOD cases, especially the *trees* and *bridge*, as shown in Figure 8. Please check our supplemental document for more results.

3.4. User study

Restored photos of industrial products such as Google Photo Scan (GPS) and Genius Scan (GS) are produced manually using their applications on the same device as the one making DIV2K-SCAN. However, different positions while taking photos may cause structural inconsistency between their scanned photos and ours. Plus, unlike scanning by a professional scanner with the bird’s eye view, scanning by a smartphone in the 3D world is more challenging because of the structural mismatch between scanned photos and the ground-truth images, even after perspective warping. The evaluation with computational similarity measurements is thus less reliable, especially MS-SSIM. To address the is-

sue, inspired by [11], we conduct a user study based on two-alternative forced-choice (2AFC) anchored by user preference on image quality and colors. Particularly, we first show an example including a scanned photo A and its ground-truth image B to rehearse about distortion, degraded color, and artifacts, then ask the participants “which photo has the highest quality?”. Each method is paired with others the same number of times. Therefore, they are fairly compared. Regarding the experimental samples, we select 120 pairs from *testset*, and half of them are centrally cropped with the size of 512×512 for easier comparison. Please check our supplemental document for the illustration. Eventually, there are 31 people participating in the experiment giving 3,720 votes in total. As a result, our work attains the highest rate of being chosen as **DPScan (SSL): 92.34%**; meanwhile, *in high-to-low probability of being chosen order*, the scores of other works are as **Pix2Pix : 68.23%** \rightarrow **OPR: 58.06%** \rightarrow **CycleGAN: 34.52%** \rightarrow **GPS: 30.81%** \rightarrow **GS: 16.05%**. This order also reflects the order of compared scores in PSNR and LPIPS perfectly on *testset 75*, as shown Table 1. However, MS-SSIM breaks the order as GPS performs better than OPR and CycleGAN. It may be because of the structural mismatch we previously mentioned. Based on the conducted user study, we come to two conclusions: 1) our semi-supervised DPScan outperforms other works in human preference on image quality, 2) we also clarify that PSNR and LPIPS are more reliable than MS-SSIM on image restoration when the misalignment is unavoidable.

4. Conclusion

We produce real-world degradation and present the DIV2K-SCAN dataset for smartphone-scanned photo restoration based on DIV2K [32]. It enables a deep neural network to be trained with supervised learning. Furthermore, we adopt the concept of GANs to learn how to degrade a high-quality image as if it were scanned by a smartphone and propose the semi-supervised Deep Photo Scan (DPScan) having two advantages: 1) semi-supervised approach training a model on both scanned and unscanned photos, 2) the designed Residual Efficient Channel Attention (RECA) Block and RECA U-Block. As a result, our semi-supervised DPScan outperforms its baseline architecture, two industrial products Google Photo Scan and Genius Scan, the previous works Old Photo Restoration [33, 34], two retrained Pix2Pix [15] and CycleGAN [47] quantitatively and qualitatively. Furthermore, the conducted user study shows that this work also outperforms others in user preference on image quality with the highest probability of being chosen. Our work, therefore, becomes a promising baseline for smartphone-scanned photo restoration.

References

- [1] Abdelrahman Abdelhamed, Stephen Lin, and Michael S Brown. A high-quality denoising dataset for smartphone cameras. In *Proceedings of the IEEE Conference on Computer Vision and Pattern Recognition*, pages 1692–1700, 2018. 2
- [2] Vijay Badrinarayanan, Alex Kendall, and Roberto Cipolla. Segnet: A deep convolutional encoder-decoder architecture for image segmentation. *IEEE transactions on pattern analysis and machine intelligence*, 39(12):2481–2495, 2017. 2
- [3] David Berthelot, Nicholas Carlini, Ian Goodfellow, Nicolas Papernot, Avital Oliver, and Colin A Raffel. Mixmatch: A holistic approach to semi-supervised learning. In *Advances in Neural Information Processing Systems*, pages 5049–5059, 2019. 2
- [4] John Canny. A computational approach to edge detection. *IEEE Transactions on pattern analysis and machine intelligence*, (6):679–698, 1986. 2, 4, 6
- [5] Ting Chen, Simon Kornblith, Kevin Swersky, Mohammad Norouzi, and Geoffrey Hinton. Big self-supervised models are strong semi-supervised learners. *arXiv preprint arXiv:2006.10029*, 2020. 2
- [6] Tao Dai, Jianrui Cai, Yongbing Zhang, Shu-Tao Xia, and Lei Zhang. Second-order attention network for single image super-resolution. In *Proceedings of the IEEE/CVF Conference on Computer Vision and Pattern Recognition (CVPR)*, June 2019. 2
- [7] Martin A Fischler and Robert C Bolles. Random sample consensus: a paradigm for model fitting with applications to image analysis and automated cartography. *Communications of the ACM*, 24(6):381–395, 1981. 4, 6
- [8] Ian Goodfellow, Jean Pouget-Abadie, Mehdi Mirza, Bing Xu, David Warde-Farley, Sherjil Ozair, Aaron Courville, and Yoshua Bengio. Generative adversarial nets. In *Advances in neural information processing systems*, pages 2672–2680, 2014. 2
- [9] Jianzhong He, Shiliang Zhang, Ming Yang, Yanhu Shan, and Tiejun Huang. Bi-directional cascade network for perceptual edge detection. In *Proceedings of the IEEE Conference on Computer Vision and Pattern Recognition*, pages 3828–3837, 2019. 2
- [10] Kaiming He, Xiangyu Zhang, Shaoqing Ren, and Jian Sun. Deep residual learning for image recognition. In *Proceedings of the IEEE conference on computer vision and pattern recognition*, pages 770–778, 2016. 4, 5, 7
- [11] Man M. Ho and Jinjia Zhou. Deep preset: Blending and retouching photos with color style transfer. In *Proceedings of the IEEE/CVF Winter Conference on Applications of Computer Vision (WACV)*, pages 2113–2121, January 2021. 9
- [12] Minh-Man Ho, Jinjia Zhou, and Yibo Fan. Respecting low-level components of content with skip connections and semantic information in image style transfer. In *European Conference on Visual Media Production*, pages 1–9, 2019. 2, 5
- [13] Man M Ho, Jinjia Zhou, Gang He, Muchen Li, and Lei Li. Sr-cl-dmc: P-frame coding with super-resolution, color learning, and deep motion compensation. In *Proceedings of the IEEE/CVF Conference on Computer Vision and Pattern Recognition Workshops*, pages 124–125, 2020. 7
- [14] Andrey Ignatov, Nikolay Kobyshev, Radu Timofte, Kenneth Vanhoey, and Luc Van Gool. Dslr-quality photos on mobile devices with deep convolutional networks. In *Proceedings of the IEEE International Conference on Computer Vision*, pages 3277–3285, 2017. 2
- [15] Phillip Isola, Jun-Yan Zhu, Tinghui Zhou, and Alexei A Efros. Image-to-image translation with conditional adversarial networks. In *Computer Vision and Pattern Recognition (CVPR), 2017 IEEE Conference on*, 2017. 2, 4, 6, 7, 8, 9
- [16] Justin Johnson, Alexandre Alahi, and Li Fei-Fei. Perceptual losses for real-time style transfer and super-resolution. In *European conference on computer vision*, pages 694–711. Springer, 2016. 3, 5, 7
- [17] Claudio Rosito Jung and Rodrigo Schramm. Rectangle detection based on a windowed hough transform. In *Proceedings. 17th Brazilian Symposium on Computer Graphics and Image Processing*, pages 113–120. IEEE, 2004. 2
- [18] Zhen Li, Jinglei Yang, Zheng Liu, Xiaomin Yang, Gwanggil Jeon, and Wei Wu. Feedback network for image super-resolution. In *Proceedings of the IEEE/CVF Conference on Computer Vision and Pattern Recognition (CVPR)*, June 2019. 2
- [19] Bee Lim, Sanghyun Son, Heewon Kim, Seungjun Nah, and Kyoung Mu Lee. Enhanced deep residual networks for single image super-resolution. In *The IEEE Conference on Computer Vision and Pattern Recognition (CVPR) Workshops*, July 2017. 6
- [20] Jae Hyun Lim and Jong Chul Ye. Geometric gan. *arXiv preprint arXiv:1705.02894*, 2017. 4
- [21] Nicolas Limare, Jose-Luis Lisani, Jean-Michel Morel, Ana Belén Petro, and Catalina Sbert. Simplest color balance. *Image Processing On Line*, 1:297–315, 2011. 8, 9
- [22] Hanxiao Liu, Andrew Brock, Karen Simonyan, and Quoc V Le. Evolving normalization-activation layers. *arXiv preprint arXiv:2004.02967*, 2020. 3, 4, 5, 7
- [23] Yun Liu, Ming-Ming Cheng, Xiaowei Hu, Kai Wang, and Xiang Bai. Richer convolutional features for edge detection. In *Proceedings of the IEEE conference on computer vision and pattern recognition*, pages 3000–3009, 2017. 2
- [24] David G Lowe. Distinctive image features from scale-invariant keypoints. *International journal of computer vision*, 60(2):91–110, 2004. 4, 6
- [25] Takeru Miyato, Toshiki Kataoka, Masanori Koyama, and Yuichi Yoshida. Spectral normalization for generative adversarial networks. *arXiv preprint arXiv:1802.05957*, 2018. 4, 5
- [26] Yassine Ouali, Céline Hudelot, and Myriam Tami. Semi-supervised semantic segmentation with cross-consistency training. In *Proceedings of the IEEE/CVF Conference on Computer Vision and Pattern Recognition*, pages 12674–12684, 2020. 2
- [27] Tobias Plotz and Stefan Roth. Benchmarking denoising algorithms with real photographs. In *Proceedings of the IEEE conference on computer vision and pattern recognition*, pages 1586–1595, 2017. 2

- [28] Xavier Soria Poma, Edgar Riba, and Angel Sappa. Dense extreme inception network: Towards a robust cnn model for edge detection. In *The IEEE Winter Conference on Applications of Computer Vision*, pages 1923–1932, 2020. 2, 4, 6
- [29] Olaf Ronneberger, Philipp Fischer, and Thomas Brox. U-net: Convolutional networks for biomedical image segmentation. In *International Conference on Medical image computing and computer-assisted intervention*, pages 234–241. Springer, 2015. 2, 3, 4, 5, 7
- [30] Xi Shen, François Darmon, Alexei A Efros, and Mathieu Aubry. Ransac-flow: generic two-stage image alignment. In *16th European Conference on Computer Vision*, 2020. 6
- [31] Richard Szeliski. Image alignment and stitching: A tutorial. *Foundations and Trends® in Computer Graphics and Vision*, 2(1):1–104, 2006. 4, 6
- [32] Radu Timofte, Shuhang Gu, Jiqing Wu, Luc Van Gool, Lei Zhang, Ming-Hsuan Yang, Muhammad Haris, et al. Ntire 2018 challenge on single image super-resolution: Methods and results. In *The IEEE Conference on Computer Vision and Pattern Recognition (CVPR) Workshops*, June 2018. 2, 4, 5, 9
- [33] Ziyu Wan, Bo Zhang, Dongdong Chen, Pan Zhang, Dong Chen, Jing Liao, and Fang Wen. Bringing old photos back to life. In *Proceedings of the IEEE/CVF Conference on Computer Vision and Pattern Recognition*, pages 2747–2757, 2020. 2, 9
- [34] Ziyu Wan, Bo Zhang, Dongdong Chen, Pan Zhang, Dong Chen, Jing Liao, and Fang Wen. Old photo restoration via deep latent space translation. *arXiv preprint arXiv:2009.07047*, 2020. 1, 2, 6, 7, 8, 9
- [35] Qilong Wang, Banggu Wu, Pengfei Zhu, Peihua Li, Wangmeng Zuo, and Qinghua Hu. Eca-net: Efficient channel attention for deep convolutional neural networks. In *Proceedings of the IEEE/CVF Conference on Computer Vision and Pattern Recognition*, pages 11534–11542, 2020. 2, 4, 5, 7
- [36] Xintao Wang, Ke Yu, Shixiang Wu, Jinjin Gu, Yihao Liu, Chao Dong, Yu Qiao, and Chen Change Loy. Esrgan: Enhanced super-resolution generative adversarial networks. In *Proceedings of the European Conference on Computer Vision (ECCV)*, pages 0–0, 2018. 2
- [37] Yaxing Wang, Salman Khan, Abel Gonzalez-Garcia, Joost van de Weijer, and Fahad Shahbaz Khan. Semi-supervised learning for few-shot image-to-image translation. In *Proceedings of the IEEE/CVF Conference on Computer Vision and Pattern Recognition*, pages 4453–4462, 2020. 2
- [38] Zhou Wang, Eero P Simoncelli, and Alan C Bovik. Multi-scale structural similarity for image quality assessment. In *The Thirty-Seventh Asilomar Conference on Signals, Systems & Computers, 2003*, volume 2, pages 1398–1402. Ieee, 2003. 3, 4, 6, 7
- [39] Saining Xie and Zhuowen Tu. Holistically-nested edge detection. In *Proceedings of the IEEE international conference on computer vision*, pages 1395–1403, 2015. 2
- [40] Xiaohua Zhai, Avital Oliver, Alexander Kolesnikov, and Lucas Beyer. S4l: Self-supervised semi-supervised learning. In *Proceedings of the IEEE international conference on computer vision*, pages 1476–1485, 2019. 2
- [41] Han Zhang, Ian Goodfellow, Dimitris Metaxas, and Augustus Odena. Self-attention generative adversarial networks. In *International Conference on Machine Learning*, pages 7354–7363. PMLR, 2019. 4, 5, 7
- [42] Richard Zhang. Making convolutional networks shift-invariant again. In *ICML*, 2019. 3, 4, 5, 7
- [43] Richard Zhang, Phillip Isola, Alexei A Efros, Eli Shechtman, and Oliver Wang. The unreasonable effectiveness of deep features as a perceptual metric. In *Proceedings of the IEEE conference on computer vision and pattern recognition*, pages 586–595, 2018. 3, 4, 6, 7
- [44] Richard Zhang, Jun-Yan Zhu, Phillip Isola, Xinyang Geng, Angela S Lin, Tianhe Yu, and Alexei A Efros. Real-time user-guided image colorization with learned deep priors. *ACM Transactions on Graphics (TOG)*, 9(4), 2017. 2
- [45] Xuaner Zhang, Qifeng Chen, Ren Ng, and Vladlen Koltun. Zoom to learn, learn to zoom. In *Proceedings of the IEEE Conference on Computer Vision and Pattern Recognition*, pages 3762–3770, 2019. 2
- [46] Yulun Zhang, Kunpeng Li, Kai Li, Lichen Wang, Bineng Zhong, and Yun Fu. Image super-resolution using very deep residual channel attention networks. In *Proceedings of the European conference on computer vision (ECCV)*, pages 286–301, 2018. 7
- [47] Jun-Yan Zhu, Taesung Park, Phillip Isola, and Alexei A Efros. Unpaired image-to-image translation using cycle-consistent adversarial networkss. In *Computer Vision (ICCV), 2017 IEEE International Conference on*, 2017. 2, 6, 7, 8, 9